

Cite this article as: Cong Jiahui, Wang Lei, Xu Yongzhen, et al. Influence of Ultrasonic Surface Rolling on Fatigue Behavior of 2D12 Aluminum Alloy[J]. Rare Metal Materials and Engineering, 2022, 51(01): 113-118.

ARTICLE

Influence of Ultrasonic Surface Rolling on Fatigue Behavior of 2D12 Aluminum Alloy

Cong Jiahui^{1,2}, Wang Lei², Xu Yongzhen¹, Hui Li²

¹ School of Mechatronics Engineering, Shenyang Aerospace University, Shenyang 110136, China; ² Key Laboratory of Fundamental Science for National Defense of Aeronautical Digital Manufacturing Process, Shenyang Aerospace University, Shenyang 110136, China

Abstract: The effects of ultrasonic rolling strengthening treatment and polishing on 2D12 aluminum alloys were investigated, and the surface hardening, residual stress, and fatigue life were studied. The residual compressive stress and gradient nano-crystalline structure can reduce the fatigue crack initiation and propagation, which play a critical role in improving fatigue performance of components. The results and analytic predictions indicate that after ultrasonic rolling strengthening treatment, the axial compressive stress and the microhardness of specimens are improved by 55% and 20%, respectively. The strengthening rule provides a guidance for strengthening process and the fatigue behavior improvement of 2D12 alloy.

Key words: ultrasonic rolling strengthening; aluminum alloys; residual stress; fatigue behavior

Aluminum alloys are widely used as components of aircrafts because of their high specific strength, corrosion resistance, and wear resistance^[1]. Generally, the fatigue damage is the main reason of fracture under cycle loading during the service period. Thus, the improvement of the fatigue properties is a critical problem in engineering.

The microstructure, surface morphology, residual stress, and surface roughness have a certain influence on the fatigue properties^[2,3]. Currently, researches are focused on the enhancement in fatigue life by the combined effects of surface nanostructure and compressive residual stresses^[4]. Because the residual stresses can increase the fatigue strength, several mechanical processes have been studied in order to introduce compressive residual stresses on the material surface. The ultrasonic strengthening treatment can cause plastic deformation of the surface material, resulting in residual compressive stress with a cold processing technique. The small grain size can raise the threshold of fatigue crack initiation and coarse grains may deflect the propagation paths of fatigue cracks by grain boundaries, thus introducing crack closure and decreasing the rate of crack growth^[5].

Usually, the fatigue cracks are initiated from surface layer

of the components. In order to improve the fatigue performance of metal components, surface strengthening treatments are considerably effective, including conventional shot peening (SP), ultrasonic shot peening (USP), laser shock peening (LSP), ultrasonic surface rolling (USR), ultrasonic impact treatment (UIT), low plasticity burnishing (LPB), and surface mechanical attrition treatment (SMAT)^[6,7].

USP can increase the resistance of materials to surface-related failures, such as fatigue and stress corrosion cracking. Some researches also show that USP is one of the most efficient techniques for increasing the fatigue life of welded components, compared with grinding, SP, and hammer peening methods^[8-10]. Marteau et al^[11] studied the surface roughness of AISI 316L steel specimens after USP with different processing parameters and obtained a linear relationship between the roughness and the fatigue performance. Lindemann et al^[12] reported that the compressive residual stresses and surface strengthening effect can be observed in the surface layer after USP. Benedetti et al^[13] studied the effect of the peening intensity on the reverse bending fatigue behavior of Al-7075-T651 alloy, and discussed the effect of roughness, strain hardening, and

Received date: January 30, 2021

Foundation item: Sponsored by Key Laboratory of Vibration and Control of Aero-propulsion System, Ministry of Education, Northeastern University (VCAME201908); Sponsored by Key Laboratory of Fundamental Science for National Defence of Aeronautical Digital Manufacturing Process (SHSYS201901)

Corresponding author: Cong Jiahui, Ph. D., Lecturer, School of Mechatronics Engineering, Shenyang Aerospace University, Shenyang 110136, P. R. China, Tel: 0086-24-89724538, E-mail: congjiahui2011@163.com

Copyright © 2022, Northwest Institute for Nonferrous Metal Research. Published by Science Press. All rights reserved.

residual stresses. Roland et al.^[14] performed tension-compression fatigue tests on 316 stainless steel after SMAT and found that the fatigue limit improves by 16%~21%. Li et al.^[15] also performed pulsating fatigue tests on stainless steel plates after SMAT and found that SMAT process can improve the fatigue strength of 400-series stainless steel with nano-crystallized surface by 13%.

USR is a mechanical surface treatment without modifying the chemical composition of the material to rapidly realize surface nano-crystallization, which also impacts the surface strengthening effect^[16-18]. As a new technique, USR combines ultrasonic frequency vibrations with the static forces, thereby achieving the advantages of SMAT, UIT, and LPB, which can improve the fatigue resistance, microhardness, and fatigue life^[19]. In addition, USR is also considered to improve the surface properties and microstructure, reduce the material failures, and ameliorate the fatigue life of materials^[20-22]. Zhang et al.^[23] investigated the fatigue performance of machine parts treated by USR which introduces a compressive residual stress field into the surface of metallic materials due to the cold working effect. Wang et al.^[24] revealed that a deformed layer with a gradient microstructure is generated near the surface treated by USR, and the microstructure changes from a coarse lamellar θ structure to ultrafine lamellar grains, ultrafine equiaxed grains, and nanograins. The deformed layer has a much higher hardness than the matrix does, which is ascribed to the grain boundary strengthening and dislocation strengthening effects. Dai et al.^[25] found that the hardness of Inconel 690 alloy is increased with decreasing the grain size. The materials of nanostructure have a higher strength and exhibit a better fatigue resistance, compared with the materials with coarse grains.

Generally, USR is a surface strengthening method superior to USP. USR exerts a better improvement in surface roughness than USP does, although the later has a more obvious degree of work hardening; USR and USP have similar residual stress distribution, but the residual stress of USR is deeper. This research focused on the influence of USR on the fatigue properties of materials, including surface hardening, residual stress, and surface profiles. The surface integrity of specimens, including microhardness, residual stress, and microstructure, was also investigated to discuss the effects of modification on surface layer of different specimens (turning, turning+surface polishing, and turning+USR).

1 Experiment

Th 2D12 aluminum alloy was used in this research, and its phase analysis was already described in Ref. [26]. The chemical composition of 2D12 aluminum alloy is shown in Table 1.

The USR experiment device is displayed in Fig. 1. The

Table 1 Chemical composition of 2D12 aluminum alloy (wt%)

Si	Fe	Cu	Mn	Mg	Zn	Ti	Al
0.2	0.3	4.1	0.4	1.5	0.1	0.1	Bal.

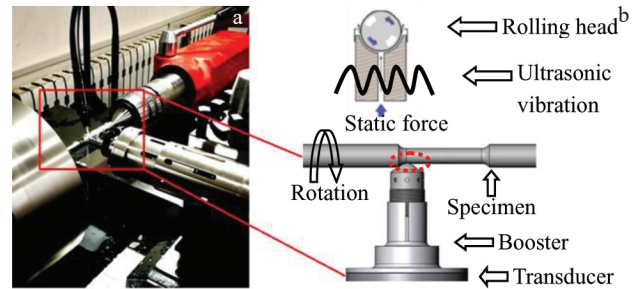


Fig.1 Appearance (a) and schematic diagram (b) of USR device

vibration amplitude was 30~40 μm with a feed speed of 5~10 mm/s. The tool tip was driven by the ultrasonic waves with a frequency of 20 kHz to achieve the high-frequency impact and the material surface was rolled under a static force.

The microstructure of 2D12 aluminum alloy was observed by optical microscope (OM). The surfaces were etched by Keller reagent (2.5vol% HNO_3 , 1.5vol% HCl , 1vol% HF , 95vol% H_2O). The microhardness was measured by the HVS-1000A microhardness tester. The load was 4.9 N with a holding duration of 12 s. The microhardness at different points was obtained, and the mean value and standard deviation of microhardness at different positions were calculated.

The residual stress profiles were determined by X-ray diffraction (XRD) at the specimen surface along the axial direction of the central position. Five points were selected along the longitudinal direction on the tensile specimen surface, and the interval of each two adjacent points was set as 8 mm, as shown in Fig.2 (point 3 was the central point of the tensile specimen). The effect of USR on the distribution of residual stress along the depth direction was also investigated.

All fatigue tests were operated on a 100 kN high frequency fatigue testing machine under the constant amplitude loading with frequency of 120 Hz and stress ratio of $R=0.06$ at room temperature in air. Low energy ion milling was used. In fatigue tests, the specimens treated by turning, turning+surface polishing, and turning+USR were named as T1, T2, and T3, respectively. The fracture morphologies of specimens were analyzed by scanning electron microscope (SEM). Fig. 3 shows the size of the 2D12 aluminum alloy specimens used in the fatigue tests.

2 Results and Discussion

2.1 Microstructure

The OM cross-sectional microstructures of specimens after polishing and after USR, i.e., T2 and T3 specimens, are shown in Fig.4 and Fig.5, respectively. It can be seen that the grain

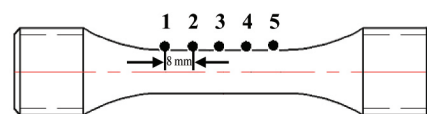


Fig.2 Schematic diagram of measurement points in residual stress test

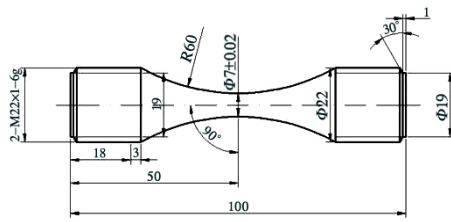


Fig.3 Schematic diagram of specimen for fatigue tests

characteristic boundary of T2 specimen is obvious and complete, while the thickness of the plastic deformation layer of T3 specimen is increased after USR and many grain boundaries are generated.

The microstructure of the surface layer of T3 specimen is finer than that of T2 specimen. The bright area in Fig. 5 represents the irregularly shaped crystals of nanostructure without sharp crystal size distribution. The refined microstructure improves the microhardness, wear resistance, and residual compressive stress, and the reduction of deformation twins indicates that the main mechanism of plastic deformation changes.

2.2 Microhardness

The microhardness at five different points of T2 and T3 specimens is shown in Fig. 6, and the average microhardness and standard deviation of microhardness are shown in Table 2.

It can be seen that after USR, the microhardness at different points is significantly improved. The average microhardness of T3 specimen is 1245 MPa, which increases by around 20% compared with that of T2 specimen, due to the increase in deformation bands and dislocation density during surface

deformation. The work hardening prevents the formation of slip bands on the specimen surface and inhibits the initiation of fatigue cracks. The increase in microhardness caused by USR treatment can improve the fatigue resistance of 2D12 aluminum alloy.

2.3 Residual stress

The detailed residual stress results of T2 and T3 specimens are shown in Table 3. The average surface residual stress and standard deviation of surface residual stress along the axial direction are shown in Table 4.

It can be found that all USR-treated specimens show compressive stress. The surface residual stress of the base material after polishing is around -173 MPa, while the T3 specimen after USR treatment shows a higher compressive residual stress of -268 MPa in average value at the surface layer. The surface residual stress along axial direction of T3 specimen increases by 55% compared with that of T2 specimen.

Fig. 7 shows the residual stress of T2 and T3 specimens along the depth direction, which exhibits the similar trend. The surface compressive residual stress is obviously increased after USR treatment.

The residual stress should be taken into consideration because it affects the fatigue performance. It can be clearly observed that the residual stress along axial direction of T3 specimens is obviously higher than that of T2 specimens, which is beneficial to the performance improvement.

2.4 Fatigue properties

The stress and fatigue life both determine the fatigue performance of specimens. The results of the applied stress (σ) and fatigue life (N , namely the number of fatigue test cycles)

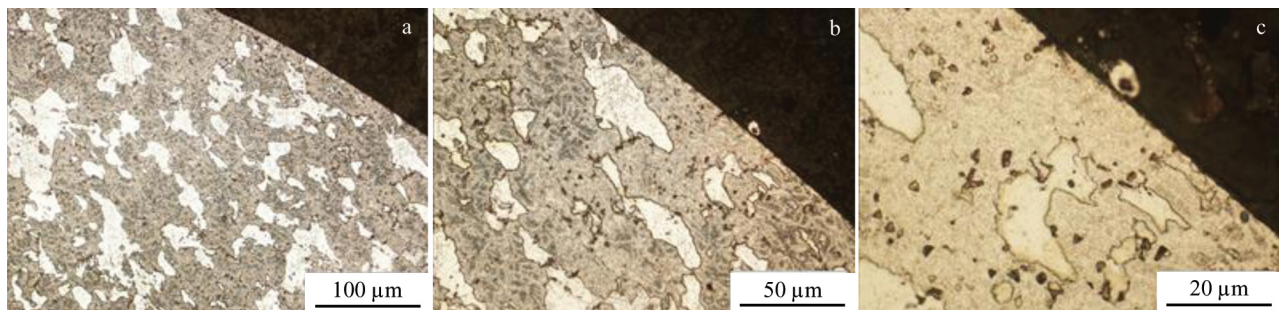


Fig.4 OM images of T2 specimen at different scales: (a) 100×, (b) 200×, and (c) 500×

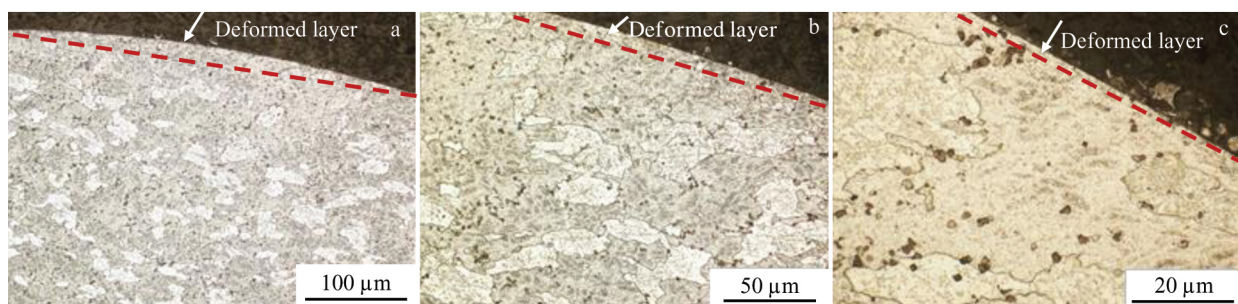


Fig.5 OM images of T3 specimen at different scales: (a) 100×, (b) 200×, and (c) 500×

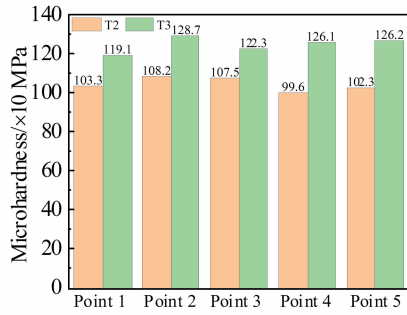


Fig.6 Microhardness at five different points of T2 and T3 specimens

Table 2 Average microhardness and standard deviation of microhardness of T2 and T3 specimens (MPa)

Specimen	Average of microhardness	Standard deviation of microhardness
T2	1042	58
T3	1245	77

Table 3 Residual stress at different points of T2 and T3 specimens (MPa)

Specimen	Point				
	1	2	3	4	5
T2-1	-194	-173	-187	-193	-201
T2-2	-188	-162	-167	-148	-180
T2-3	-183	-121	-157	-159	-176
T3-1	-294	-257	-253	-239	-269
T3-2	-286	-277	-252	-243	-269
T3-3	-277	-254	-259	-269	-327

Table 4 Average residual stress and standard deviation of residual stress along axial direction of T2 and T3 specimens (MPa)

Specimen	Average residual stresses	Standard deviation of residual stress
T2	-173	20.941
T3	-268	22.344

are represented in Table 5, and the related σ - N curves are shown in Fig.8. Therefore, the fatigue strength corresponding to the number of fatigue test cycles can be obtained.

The relationship between the fatigue life N and the stress range $\Delta\sigma$ can be expressed by Eq.(1):

$$m \lg \Delta\sigma + \lg N = \lg C \quad (1)$$

where C and m are material constants. The peak stress σ_{\max} can be calculated through stress range and stress ratio.

The fitting equations of σ_{\max} - N curves are shown in Table 6, and therefore C and m can be calculated, according to Eq.(1).

The fatigue limit of T3 specimen is about 10 and 1.5 times higher than that of the T2 specimen at the stress amplitude of 370 and 450 MPa, respectively. Because of different surface

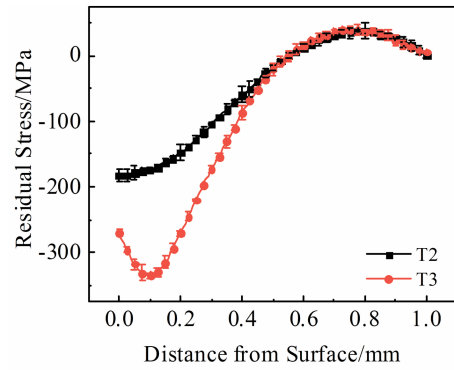


Fig.7 Residual stress of T2 and T3 specimens along the depth direction

Table 5 Fatigue test results of T1, T2, and T3 specimens

Specimen	Stress/MPa	$N/\times 10^3$ cycle					$N_{50}/\times 10^3$ cycle
		15.6	21.7	24.8	17.2	23.6	
T1	450	15.6	21.7	24.8	17.2	23.6	20.253
	370	174.9	137.6	190.4	134.2	137.7	153.304
	320	383.8	818.7	497.8	626.3	339.8	506.359
T2	450	26.9	22.2	22.4	47.5	36.3	29.689
	370	307.5	191.2	184.3	243.6	233.7	228.055
	320	8620.8	714.2	$>10^4$	$>10^4$	$>10^4$	-
T3	450	44.3	64.4	65.3	27.0	22.9	40.953
	370	297.6	2596.4	2633.1	1517.5	3429.6	1603.130
	320	3429.7	4669.0	6479.9	9190.2	$>10^4$	-

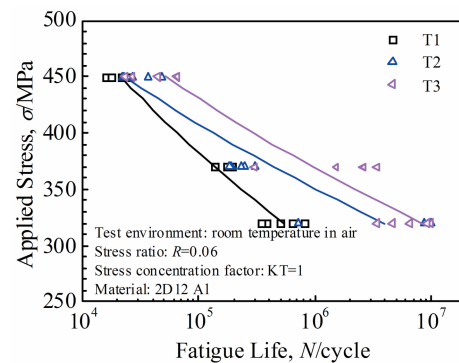


Fig.8 Applied stress σ -fatigue life N curves of T1, T2, and T3 specimens

Table 6 Fitting equations of σ_{\max} - N curves of T1, T2, and T3 specimens

Specimen	Fitting equation
T1	$\lg N = 29.513 - 9.4921 \lg \sigma_{\max}$
T2	$\lg N = 44.553 - 15.1521 \lg \sigma_{\max}$
T3	$\lg N = 44.433 - 14.9731 \lg \sigma_{\max}$

treatments, the stress of T3 specimen is higher than that of T1 and T2 specimens under the same condition, which indicates

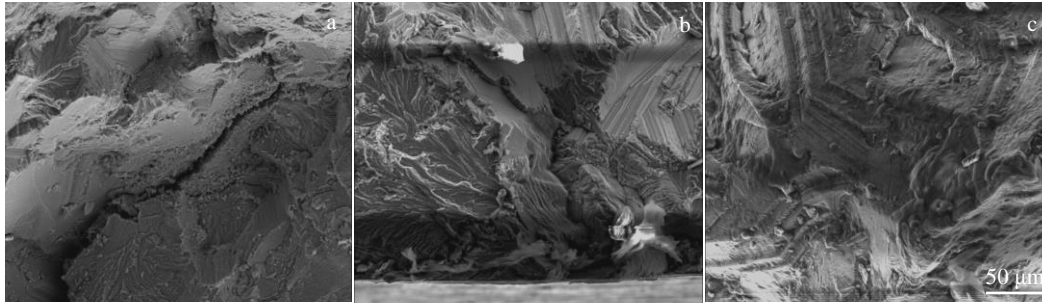


Fig.9 LCF fracture surfaces of T1 (a), T2 (b), and T3 (c) specimens

that fatigue performance of the 2D12 aluminum alloy is increased by USR treatment.

The crack initiation mechanism of specimen surface is changed after USR treatment. Most cracks are difficult to propagate due to the compressive stress and the improvement in surface roughness, thus leading to the increase in fatigue life, which agrees with the material fatigue fracture theory. The improvement of low cycle fatigue (LCF) life may be ascribed to the increase in the resistance against crack initiation resulting from USR, i. e., the combined effect of surface layer of nanostructure and the residual compressive stress induced by USR improves the fatigue life of material.

2.5 Fracture surface

The fatigue fracture of specimens consists of the crack initiation, crack propagation, and final rupture, while the crack initiation accounts for 70%~80% of the entire fatigue life. Thus, the characteristics of crack initiation should be seriously concerned. The fracture morphologies of 2D12 aluminum alloys were obtained under the maximum cyclic stress of 450 MPa by SEM, as shown in Fig.9.

The typical LCF fractography of specimens shows that the fatigue source of T1 specimen is initiated on the specimen surface, while that of T3 specimen appears at a deeper position from the specimen surface, which indicates that USR can cause the movement of the crack initiation site towards the subsurface direction. This phenomenon is due to the fact that the compressive residual stress can make the micro-cracks grow slowly.

3 Conclusions

1) The ultrasonic surface rolling (USR) treatment can improve the surface microstructure into the fine nanostructure in 2D12 aluminum alloy. A highly deformed surface layer of nanostructure is generated in alloys after USR treatment. Thus, the fatigue crack is prevented to a certain extent.

2) The axial compressive stress of USR-treated specimen (268 MPa) is significantly improved by 55%, compared with that of specimen before USR treatment. USR process can cause high residual stress and surface work hardening effect, so the metallic materials after USR treatment have better fatigue performance.

3) The microhardness of USR-treated specimens is obviously increased. The average microhardness of USR-

treated specimen is 1245 MPa, which is improved by about 20% compared with that of specimen after polishing.

4) The better fatigue life and fatigue performance can be obtained by USR treatment under the same stress condition. The fatigue limit of USR-treated specimens is much higher than that of the specimen after polishing. The enhancement in fatigue life is due to the surface of nanostructure and compressive residual stress resulting from USR treatment.

References

- 1 Tolga D, Costas S. *Materials & Design*[J], 2014, 56: 862
- 2 Luo Sihai, Nie Xiangfan, Wang Xuede et al. *Rare Metal Materials and Engineering*[J], 2017, 46(12): 3682
- 3 Chen Chao, Chen Furong, Zhang Huijing. *Rare Metal Materials and Engineering*[J], 2018, 47(9): 2637
- 4 Liu C S, Liu D X, Zhang X H et al. *Surface and Coatings Technology*[J], 2019, 370: 24
- 5 Dai S J, Zhu Y T, Huang Z W. *Vacuum*[J], 2016, 125: 215
- 6 He Bolin, Yu Yingxia, Xia Songsong et al. *Rare Metal Materials and Engineering*[J], 2017, 46(1): 17
- 7 Liu D, Liu D X, Zhang X H et al. *International Journal of Fatigue*[J], 2020, 131: 105 340
- 8 Wang C, Shen X J, An Z B et al. *Materials & Design*[J], 2016, 89: 582
- 9 Wu X L, Yang M X, Yuan F P et al. *Acta Materialia*[J], 2016, 112: 337
- 10 Bagherifard S, Fernandez-Pariente I, Ghelichi R et al. *International Journal of Fatigue*[J], 2014, 65: 64
- 11 Marteau J, Bigerelle M, Mazeran P E et al. *Tribology International*[J], 2015, 82: 319
- 12 Lindemann J, Buque C, Appel F. *Acta Materialia*[J], 2006, 54(4): 1155
- 13 Benedetti M, Fontanari V, Scardi P et al. *International Journal of Fatigue*[J], 2009, 31(8-9): 1225
- 14 Roland T, Reirant D, Lu K et al. *Materials Science and Engineering A*[J], 2007, 445-446: 281
- 15 Li Y, Hou L F, Wei Y H et al. *Surface and Coatings Technology* [J], 2017, 309: 462
- 16 Li L, Kim M, Lee S et al. *Surface and Coatings Technology*[J], 2016, 307: 517

- 17 Mordyuk B N, Karasevskaya O P, Prokopenko G I. *Materials Science and Engineering A*[J], 2013, 559: 453
- 18 Liu M, Li J Y, Ma Y et al. *Surface and Coatings Technology*[J], 2016, 289: 94
- 19 Xu Xingchen, Liu Daoxin, Zhang Xiaohua et al. *International Journal of Fatigue*[J], 2019, 125: 237
- 20 Pour-Ali S, Kiani-Rashid A R, Babakhani A. *Vacuum*[J], 2017, 144: 152
- 21 Ye Y, Kure-Chu S Z, Sun Z et al. *Materials & Design*[J], 2018, 149: 214
- 22 Liu Yu, Zhao Xiaohui, Wang Dongpo. *Materials Science and Engineering A*[J], 2014, 600: 21
- 23 Zhang Meng, Deng Jia, Liu Zhihua et al. *International Journal of Mechanical Sciences*[J], 2019, 163: 105 144
- 24 Wang Zhen, Gao Chaofeng, Liu Zhongqiang et al. *Materials Science and Engineering A*[J], 2020, 772: 138 696
- 25 Dai Shijuan, Zhu Yuntian, Huang Zhaowen. *Vacuum*[J], 2016, 125: 215
- 26 Hui Li, Yang Linqing, Wang Lei et al. *China Surface Engineering*[J], 2016, 29(6): 15 (in Chinese)

超声滚压强化对2D12铝合金疲劳性能的影响

丛家慧^{1,2}, 王 磊², 徐永臻¹, 回 丽²

(1. 沈阳航空航天大学 机电工程学院, 辽宁 沈阳 110136)

(2. 沈阳航空航天大学 航空制造工艺数字化国防重点学科实验室, 辽宁 沈阳 110136)

摘 要: 通过对比分析2D12铝合金超声强化试样与抛光试样的疲劳性能, 对表面硬化、残余应力和疲劳寿命进行了研究。残余压应力和梯度纳米晶结构对改善构件的疲劳性能起着至关重要的作用, 可以有效减少疲劳裂纹的萌生和扩展。实验及分析预测结果表明, 试样经超声强化后, 轴向压应力提高了55%, 显微硬度提高了20%。通过对表面强化规律的研究, 为2D12铝合金的强化工艺和疲劳性能的影响提供了指导。

关键词: 超声滚压强化; 铝合金; 残余应力; 疲劳性能

作者简介: 丛家慧, 女, 1980年生, 博士, 讲师, 沈阳航空航天大学机电工程学院, 辽宁 沈阳 110136, 电话: 024-89724538, E-mail: congjiahui2011@163.com